Journal of Hepatocellular Carcinoma

Dovepress
Taylor & Francis Group

Open Access Full Text Article

ORIGINAL RESEARCH

Integrative Single-Cell and Spatial Transcriptomic Analysis Reveals MAIT Cell Dysfunction in Relapsed HCC

Geon Woo Park[1–3,*], Hayoung Jang[1,2,*], Thuy Nguyen-Phuong[4,*], Hyunsung Nam[2], Chung-Gyu Park[1–5], Gwang Hyeon Choi[6], Sook-Hyang Jeong[6,7], Jin-Wook Kim[6,7], Chang Jin Yoon[8–10], Jae Hwan Lee[8–10], Hyun Je Kim[1–3,5,11,12]

[1]Department of Biomedical Sciences, Seoul National University Graduate School, Seoul, Republic of Korea; [2]Department of Microbiology and Immunology, Seoul National University College of Medicine, Seoul, Republic of Korea; [3]Cancer Research Institute, Seoul National University, Seoul, Republic of Korea; [4]Transplantation Research Institute, Medical Research Center, Seoul National University, Seoul, Republic of Korea; [5]PB Immune Therapeutics Inc, Seoul, Republic of Korea; [6]Departments of Internal Medicine, Seoul National University Bundang Hospital, Gyeonggi-do, Republic of Korea; [7]Departments of Internal Medicine, Seoul National University College of Medicine, Seoul, Republic of Korea; [8]Department of Radiology, Seoul National University Bundang Hospital, Gyeonggi-do, Republic of Korea; [9]Department of Radiology, Seoul National University College of Medicine, Seoul, Republic of Korea; [10]Institute of Radiation Medicine, Seoul National University Medical Research Center, Seoul, Republic of Korea; [11]Interdisciplinary Program in Artificial Intelligence (IPAI), Seoul National University, Seoul, Republic of Korea; [12]Genomic Medicine Institute, Seoul National University Medical Research Center, Seoul, Republic of Korea

*These authors contributed equally to this work

Correspondence: Jae Hwan Lee, Department of Radiology, Seoul National University Bundang Hospital, Gyeonggi-do, Republic of Korea, Tel +82-31-787-7619, Fax +82-31-787-4011, Email lzhwanmd@gmail.com; Hyun Je Kim, Department of Biomedical Sciences, Seoul National University Graduate School, Seoul, Republic of Korea, Tel +82-2-740-8307, Email hjkim0518@gmail.com

Purpose: Hepatocellular carcinoma (HCC) frequently recurs after curative treatment, and the tumor immune microenvironment plays an important role in disease progression. However, the role of mucosal-associated invariant T (MAIT) cells in relapsed HCC remains poorly understood. This study aimed to characterize transcriptional and spatial features of MAIT cells in relapsed HCC and their association with malignant hepatocyte phenotypes.

Patients and Methods: Tumor samples from primary (n = 3) and relapsed (n = 2) HCC patients were analyzed using paired single-cell RNA sequencing (scRNA-seq) and spatial transcriptomics. scRNA-seq data (49,229 cells) were processed using Seurat with standard quality-control thresholds, followed by Harmony batch correction and unsupervised clustering. Malignant hepatocytes were identified by copy-number variation inference. Spatial transcriptomic data from 35 regions of interest were normalized and deconvolved using scRNA-seq–derived reference profiles. Independent validation was performed using a public HCC scRNA-seq dataset.[1.]

Results: Integrated analyses revealed distinct tumor microenvironmental features in relapsed HCC. Relapsed tumors showed increased representation of malignant hepatocytes with elevated cancer stemness–related transcriptional signatures compared with primary tumors (1.18-fold increase, $p < 0.0001$), which was spatially supported by enrichment in tumor regions (1.10-fold increase, $p \leq 0.05$). Within the T/NK compartment, MAIT cells were significantly enriched in relapsed tumor regions (2.71-fold increase, $p \leq 0.05$). Transcriptomic profiling identified distinct MAIT cell states between primary and relapsed HCC, with relapsed MAIT cells displaying dysfunctional phenotype. Cell–cell interaction analysis suggested enhanced ligand–receptor interactions between MAIT cells and malignant hepatocytes in relapsed tumors. In the TCGA LIHC cohort, high relapsed MAIT cell signature scores were associated with poorer overall survival (HR = 1.52, $p \leq 0.05$).

Conclusion: Relapsed HCC is characterized by enhanced malignant hepatocyte stemness and altered MAIT cell states within the tumor microenvironment. These findings suggest an association between MAIT cell dysregulation and relapse-specific tumor biology, warranting further functional investigation.

Keywords: hepatocellular carcinoma, tumor microenvironment, tumor-infiltrating lymphocytes, mucosal-associated invariant t cells

https://doi.org/10.2147/JHC.S575861
Received: 21 October 2025
Accepted: 16 January 2026
Published: 2 February 2026

Introduction

Hepatocellular carcinoma (HCC), representing nearly 80% of liver cancer cases, is the 6th most common cancer and 3rd leading cause of cancer-related death worldwide.[1,2] Its high recurrence rate (up to 88%) and limited treatment efficacy underscore the need for better therapeutic strategies.[3] The aggressive nature of HCC highlights the need for deeper cellular and molecular investigations.

Tumor heterogeneity comprises diverse cells, including cancer, immune cells (T and B cells, macrophages), and non-immune cells (fibroblasts and endothelial cells), contributing to immunotherapy resistance, recurrence, and poor outcomes.[5,6] Recent studies have highlighted the diversity of immune subsets within the HCC tumor microenvironment (TME) across different disease stages, including macrophages, dendritic cells, regulatory T cells, and CD8+ T cells.[6–8] However, many existing studies have focused on primary tumors and the mechanism by which microenvironmental differences contribute to HCC recurrence remains unclear.

Mucosal-associated invariant T (MAIT) cells, an MR1-restricted innate-like T cell subset, constitute up to 45% of intrahepatic T cells in healthy liver.[9] Although MAIT cells are increasingly recognized as key regulators of tissue immunity and inflammation, their role in HCC progression remains unclear.[10] Previous studies have reported increased infiltration and functional impairment of MAIT cells in HCC tumors, correlating with poor clinical outcomes.[11,12] In contrast, other analyses using bulk transcriptomic data have associated higher MAIT cell–related gene signatures with improved survival.[13] These apparently conflicting observations likely reflect the phenotypic heterogeneity of MAIT cells, which can adopt effector-like, dysfunctional/exhausted, or proliferative states depending on local microenvironmental cues.[13] Importantly, tumor-infiltrating MAIT cells often exhibit features of activation-associated dysfunction, including upregulation of inhibitory receptors and reduced cytotoxic capacity, suggesting that their functional state rather than abundance alone may be critical.

Despite growing interest in MAIT cells in primary HCC, their molecular characteristics in relapsed HCC remain poorly characterized. In particular, it is unknown whether MAIT cells undergo relapse-specific transcriptional reprogramming, whether such changes are spatially restricted to tumor regions, and how MAIT cells interact with tumor cells within the relapsed TME. These questions are biologically important because relapsed HCC develops in an immune landscape that has been reshaped by prior treatments and tumor evolution, which may profoundly alter immune cell states and tumor–immune interactions.[14] Therefore, findings derived from primary HCC cannot be directly extrapolated to relapsed disease.

Spatial transcriptomics offers a unique opportunity to address these unresolved questions by preserving tissue architecture and enabling the analysis of transcriptional programs within defined tumor and adjacent non-tumor regions. To date, however, spatially resolved immune profiling of relapsed HCC particularly focused on MAIT cells has been largely unexplored. Integrating spatial transcriptomics with single-cell RNA sequencing (scRNA-seq) allows for both high-resolution cell state identification and spatial contextualization of immune-tumor interactions, providing insights not achievable with either approach alone.

Based on these considerations, we hypothesized that relapsed HCC is characterized by distinct tumor microenvironmental features, including relapse-specific changes in MAIT cell abundance, phenotype, and spatial distribution. To test this hypothesis, we performed integrated scRNA-seq and NanoString GeoMx spatial transcriptomic analyses on biopsy samples from independent cohorts of primary and relapsed HCC patients. By combining single-cell resolution with spatial context and validating key observations in external public datasets, this study aims to define relapse-associated immune and tumor features, with a particular focus on MAIT cell dysregulation and its potential association with malignant hepatocyte stemness in relapsed HCC.

Materials and Methods

Patient Samples

This research received ethical approval from the Institutional Review Board of Seoul National University Bundang Hospital (B-2112-727-302), and all participants provided written informed consent. All the procedures complied with the principles of the Declaration of Helsinki. Five individuals diagnosed with HCC at Seoul National University Bundang

Hospital (March 2022–November 2023) were included. Diagnosis was based on the criteria outlined by the Korean Liver Cancer Study Group and the National Cancer Center Korea Practice Guideline for the Management of HCC.[15]

Among the five patients, three had primary HCC, while two had relapsed HCC. A single interventional radiologist with 10 years of experience (J.H.L.) reviewed each target lesion using ultrasound to confirm its suitability for radiofrequency ablation. Immediately before ablation, the same radiologist performed 3–4 percutaneous core-needle biopsy passes of the target lesion under real-time ultrasound guidance (Aplio i700, Canon Medical Systems, Tokyo, Japan). These biopsies yielded 2–3 fresh liver tumor samples (10–12 mm) per patient, using a 17-gauge core biopsy device (ACECUT, TSK Laboratory, Tokyo, Japan). None of the patients exhibited clinical or biochemical evidence of acute liver injury at the time of tissue collection. Because biopsies are not routinely performed in all cases of recurrent HCC particularly when radiological diagnosis is sufficient the availability of relapsed HCC biopsy samples was limited, rendering these samples particularly valuable for integrative molecular analyses.

Sample Processing

Tissue samples were transported in Roswell Park Memorial Institute 1640 medium supplemented with 10% Fetal Bovine Serum (FBS). A portion comprising 25% of the liver biopsy samples from the same patient was processed into formalin-fixed, paraffin-embedded blocks for hematoxylin and eosin (H&E) staining and spatial transcriptomics analysis. Tissue samples were fixed in 4% paraformaldehyde solution (P0117CD, BYLABS, Korea) at room temperature for 24 hours, followed by paraffin embedding. Sections were cut to a thickness of 4 μm. Remaining tissues were used for the scRNA-seq analysis.

H&E Staining

The sections were stained with hematoxylin and eosin (H&E) using an automatic stainer (ST5010, Leica, Germany). Deparaffinization was performed in xylene for 10 minutes, repeated four times. Dehydration was performed in 100% ethanol for 1 minute (twice), 95% ethanol for 1 minute (twice). Sections were then rinsed and dried. Hematoxylin staining was performed for 7 minutes, followed by rinsing. Sections were treated with 1% HCl for 5 minutes, rinsed, stained with eosin for 3 seconds, and then rinsed. Dehydration was performed twice using 95% ethanol for 10 seconds (twice), followed by 100% ethanol for 10 seconds (twice). Clearing was performed in xylene for 10 seconds (three times). Finally, slides were mounted using an automated glass cover slipper (CV5030, Leica, Germany) and scanned using a slide scanner (SCN400 F, Leica, Germany).

Spatial Transcriptomic Analysis

Tissue Preparation

Slides were baked at 60°C for 30 minutes and processed for deparaffinization, rehydration, antigen retrieval, RNA exposure, and post-fixation. Slides were incubated overnight at 37°C with RNA probe mix in a hybridization chamber. After washing, tissues were incubated at room temperature for 1 hour with morphological markers including SYTO 13 (GeoMx Nuclear Stain Morphology Kit, 1:10), Alexa Fluor 647-conjugated CD3e (NBP2-54392AF647, Novus, USA, 1:100), PE-conjugated CD34 (AB18228, Abcam, UK, 1:100), and Alexa Fluor 532–conjugated pan-Cytokeratin (NBP2-33200AF532, Novus, USA, 1:100).

Regions of Interest (ROI) Selection & Collection

Slides were uploaded to the Digital Spatial Profiling (DSP) instrument, and ROIs were selected based on fluorescence signals from specific markers, including CD3 (T cells), CD34 (tumor marker, known for its role in angiogenesis in HCC), and pan-cytokeratin (epithelial cells). Tumor regions were selected based on morphological features observed in H&E staining and areas of high CD34 expression using immunofluorescence (IF) staining. The selected ROIs were exposed to UV light, and the photocleaved oligos were collected and hybridized using GeoMx software.

Library Preparation & Sequencing

PCR was performed using the GeoMx Seq Code Primer Plate and PCR Master Mix (NanoString, Seattle, WA), and ROI-derived products were collected, pooled, and purified according to the manufacturer's instructions. Library quality was assessed prior to sequencing, and libraries were sequenced on a NovaSeq 6000 platform (Illumina). To minimize

potential sources of technical bias, all GeoMx experiments were conducted by the same operator using identical equipment, reagents, and protocols across all samples. Library preparation strictly followed the manufacturer's recommended workflow without protocol modification, ensuring consistency between samples and reducing batch-related technical variation.

Sequencing Data Processing & Analysis

FASTQ files were processed using the GeoMx NGS pipeline to generate count matrices. Quality control (QC) was performed using the addPerROIQC function from the standR package. Genes with low expression (defined as counts <5) in more than 90% of ROIs were removed. ROI-level QC was applied by excluding regions with <200 nuclei. After filtering, count data were normalized using the trimmed mean of M-values (TMM) method implemented in standR. Differential expression between tumor and non-tumor ROIs was performed using the limma package. Cell type deconvolution was conducted using the SpatialDecon R library, with a custom expression reference generated from our scRNA-seq dataset using the create_profile_matrix function.

Single Cell RNA Sequencing

Cell Isolation

The remaining tissue was rinsed with PBS and incubated with Liberase (5401119001, Roche, Switzerland). Tissue was minced and incubated at 37°C for 30 minutes, with gentle agitation every 10 minutes. After incubation, the sample was pipetted 10 times. The cell suspension was filtered through a 70 μm cell strainer and collected into FBS-containing tube. Centrifuged at 60g for 1 minute at 4°C without brake. Supernatant was centrifuged at 500g for 5 minutes at 4°C. Cells were resuspended in CELLBANKER 1 (11910, ZENOAQ, JAPAN) and cryopreserved in liquid nitrogen.

Library Preparation & Sequencing

Cryopreserved cells were thawed and processed into single-cell suspensions. Cell viability and cell counts were assessed prior to library preparation, and 40,000 cells were loaded into each Gel Bead-in-Emulsion (GEM) for all samples to ensure consistency and minimize technical variability across conditions. Single-cell libraries were prepared using the Chromium Next GEM Single Cell 5′ Kit v2 (10x Genomics, Pleasanton, CA), following the manufacturer's instructions without deviation. After GEM generation, samples underwent post-GEM cleanup and cDNA amplification. cDNA quality and concentration were evaluated, and PCR amplification cycles were adjusted based on measured cDNA input to avoid amplification bias. Final libraries underwent quality control prior to sequencing on a NovaSeq 6000 platform (Illumina).

Sequencing Data Processing

Cell Ranger pipeline (v 7.1.0) was used to align reads and generate gene-cell unique molecular identifier (UMI) matrix. R package SoupX was used to remove ambient RNA. Seurat (v5.1.0) was used to read scRNA-seq matrices. Features detected in <3 cells and cells with <200 genes or >10% mitochondrial genes were excluded. Doublets were removed by using the scDblFinder package (version 1.18). Gene expression levels were normalized with "NormalizedData" function. Batch effects arising from individual patients and sequencing runs were corrected using Harmony (v1.2.4). Each sample was treated as a separate batch. Harmony integration was run on the top 20 principal components from PCA with default parameters (theta=2, lambda=1) to align cells across batches while preserving biological variability.

Cell Clustering and Annotation

Principal component analysis (PCA) was performed on scRNA-seq data using the RunPCA function in Seurat, and the top 20 PCs were used for downstream dimensionality reduction with UMAP. Unsupervised clustering was performed using FindNeighbors followed by FindClusters with the Louvain algorithm and a resolution parameter of 1.2. Analyses were repeated with different random seeds to ensure robustness of cluster assignments. Clusters exhibiting highly similar canonical marker expression profiles were manually merged to improve biological interpretability. Cell types were annotated based on canonical markers, and cluster-specific markers were identified using FindAllMarkers with min.pct = 0.25. Scanpy was used for UMAP and heatmap visualization.

Differentially Expressed Genes Analysis

DEGs were identified using FindMarkers function of the Seurat package. Filtered with adjusted p-value <0.05 and log2 fold change > 0.5. MAIT cell DEGs between the primary and relapsed tumors were visualized using EnhancedVolcano. The R package clusterProfiler was used for GO (Gene Ontology) analysis of the DEGs respectively.

Copy Number Variation (CNV) Analysis in scRNA-Seq

CNV was estimated using inferCNV and Copykat R packages. Malignant cells were identified based on Copykat result. InferCNV was run with 10x default parameters using myeloid, B, and TNK cells as references.

Cell-to-Cell Interaction Analysis

To analyze interactions between malignant hepatocytes and T-cell, we used CellPhoneDB with normalized count data as an input. Significant ligand-receptor pairs were filtered with P-value of < 0.05.

The Cancer Genome Atlas (TCGA) Database Analysis

Gene expression profiles and clinical information for hepatocellular carcinoma (HCC) cohorts were obtained from The Cancer Genome Atlas (TCGA) and UCSC Xena using the TCGAbiolinks R package. Patients were stratified into high- and low-risk groups based on the median of the average expression values of predefined gene signatures, including cancer stemness or MAIT cell signature genes. Kaplan–Meier survival analysis was conducted using the survival and Survminer R packages to assess differences in overall survival between the groups. Multivariate Cox proportional hazards analysis was performed and visualized using forestmodel Package.

Enrichment Analysis

Gene Set Enrichment Analysis (GSEA) of the Wnt signaling pathway (MSigDB, M77) was performed using fgsea on DEGs between tumor regions in the spatial transcriptomic data. In scRNA-seq, cancer stemness and Wnt pathway scores for malignant hepatocytes were calculated using AddModuleScore in Seurat, with stemness genes from CancerSEA. AUCell was used to assess enrichment of MAIT cells, and normal/malignant hepatocytes in spatial data. The MAIT cell signature was defined from TNK subsets in scRNA-seq using FindAllMarkers (logFC > 1.5, adjusted P < 0.05). Primary and relapsed MAIT signatures combined top 50 cluster DEGs and top 70 DEGs between primary vs relapsed tumors. The hepatocyte signatures were similarly derived (logFC > 2.5, adjusted p < 0.05).

Public Data Analysis

Public single cell RNA sequencing data of patients with HCC were obtained from CNP0000650 (CNGB Sequence Archive).[6] This dataset contains scRNA-seq profiles from tumor regions and adjacent non-tumor liver tissues of 18 HCC patients, including 12 primary HCC and 6 relapsed HCC cases. Raw count matrices were reprocessed using a workflow closely aligned with the original study. Features detected in <3 cells and cells with <200 genes or >10% mitochondrial genes were excluded. For the clustering of total cells, the top 20 PCs were selected with a resolution parameter equal to 0.8. For the clustering of T/NK population, harmony integration was run on the top 15 principal components from PCA with default parameters (theta=2, lambda=1) with a resolution parameter equal to 1.5. Cancer stemness scoring in hepatocytes, signature scoring of T/NK cell subsets identified in our cohort within the public T/NK cell population, and scoring of genes upregulated in relapsed MAIT cells in cluster 15 were all performed with AddModuleScore in Seurat. The signature gene sets for each T/NK subset in our cohorts were defined from TNK subsets in our scRNA-seq data using FindAllMarkers (logFC > 1.0, adjusted P < 0.05).

Statistical Analysis

All statistical analyses were performed using R version 4.4.0 and GraphPad Prism 9. Data distribution was assessed using standard normality tests (Shapiro–Wilk and Kolmogorov–Smirnov tests). For comparisons between two groups, unpaired differences were analyzed using a *t*-test for normally distributed data or Mann–Whitney *U*-test for non-normally distributed data. Statistical significance was set at P < 0.05.

Results

Distinct Tumor Microenvironment Heterogeneity Between Primary and Relapsed HCC Patients

Primary and relapsed HCCs have been shown to exhibit distinct differences in the TME, which is closely linked to tumor relapse.[6,16] To investigate the distinct TME and its cellular composition between primary and relapsed HCC, we performed scRNA-seq on tumor tissues collected from patients with primary and relapsed HCC (Table 1 and Figure 1A). Through scRNA-seq, the major cellular components of the tumor tissue were identified using canonical markers, including hepatocytes (ALB, SERPINA1, and KRT18), T/NK cells (TRAC, CD3D, and NKG7), myeloid cells (CD68, CD14, and LYZ), B cells (CD79A, MS4A1, and JCHAIN), endothelial cells (PECAM1, PLVAP, and VWF), and fibroblasts (COL1A1, COL1A2, and ACTA2) (Figure 1B, C, Supplementary Figure 1A and B, and Supplementary Table 1).

In addition, we profiled the whole transcriptome of tumor and non-tumor regions from the same HCC patient samples analyzed by scRNA-seq, using the GeoMx® DSP WTA assay, which preserves the spatial context of the cellular components within the TME (Figure 1A). We obtained 35 ROIs from 5 patients with HCC. Tumor regions were identified based on morphology observed in H&E staining and upregulated CD34 expression, a well-established marker for angiogenesis in HCC, using IF staining (Figure 1D and Supplementary Figure 1C).[17] To compare differences of cellular composition in tumor tissue between primary and relapsed HCC, we performed deconvolution analysis for the spatial transcriptomics data. The custom cell profile matrix for deconvolution was constructed based on the gene expression patterns identified in the paired scRNA-seq data (Supplementary Figure 1D). Using this matrix, we quantified the abundance of cell populations in spatial transcriptomic data (Figure 1E and Supplementary Table 2). Comparison of cell cluster frequencies between primary and relapsed tumors showed significant enrichment of hepatocytes (1.59-fold change than primary tumor, $p<0.0001$), which may include malignant cells, particularly in the relapsed tumor region (Figure 1F). This enrichment was observed together with decreased frequencies of T/NK and fibroblast clusters (Supplementary Figure 1E).

HCC arises from hepatocytes and undergoes progressive malignant transformation during its development. Malignant hepatocytes show distinct characteristics, such as upregulated proliferation, invasion, and immune escape, accompanied by genetic, epigenetic, and alterations.[18,19] These findings necessitate a more detailed investigation of the hepatocyte cluster to elucidate the increased hepatocytes in relapsed HCC.

Enhanced Stemness Properties of Malignant Hepatocytes in Relapsed HCC

We used Copykat, a tool designed to estimate genomic copy number profiles, to define malignant cells among the total cells from scRNA-seq data (Supplementary Figure 2A).[20] Consistent with expectations, only the hepatocyte cluster consisted of malignant cells (Figure 2A). We confirmed that malignant hepatocytes exhibited aberrant CNV profiles compared with normal reference cells (Figure 2B). To compare the enrichment of malignant hepatocytes in tumor tissues between primary and relapsed HCCs, we established transcriptional signatures that distinguished normal and malignant hepatocytes from scRNA-seq data (Supplementary Figure 2B). Scoring these gene signatures for spatial transcriptomic data revealed significant enrichment of malignant hepatocytes in the relapsed tumor region (1.10-fold change than primary tumor, $p\leq0.05$), whereas normal hepatocytes showed no substantial difference (Figure 2C and Supplementary Table 3).

Recent advancements in scRNA-seq technology have demonstrated that cancer cells within tumors exhibit heterogeneity and exist in diverse functional states.[21] DEG analysis of the malignant hepatocytes demonstrated distinct gene expression patterns between primary and relapsed tumors. Malignant hepatocytes in relapsed tumors showed significantly upregulated expression of CXCL2, EGFR, and CD44, which are associated with cancer stemness (Figure 2D). When we estimated the cancer stemness score using the CancerSEA database, malignant hepatocytes in relapsed tumors exhibited upregulated stemness properties (1.18-fold change than primary tumor, $p<0.0001$) (Figure 2E and Supplementary Table 4).[22] They also showed upregulated Wnt signaling pathway, a pathway supporting cancer stemness and hyperproliferation of cancer cells in HCC ($p<0.0001$) (Supplementary Figure 2C and Supplementary Table 5).[23] Additionally, GSEA analysis of spatial transcriptomics data further confirmed Wnt signaling enrichment in the relapsed tumor region compared to the primary tumor region (NES=−1.66, p value=0.013) (Supplementary Figure 2D). Stem cell-like phenotype or cancer stemness has been suggested as association

Table 1 Patients Demographics

Sex	Age	Tumor Type	Time Interval (day)	Previous Treatment	Etiology	Presence Of LC	Child Pugh Score	Tumor Size (cm)	Macrovascular Invasion	AFP (ng/mL)	scRNA-seq Batch	Spatial Transcriptomics Batch
Male	58	Recurred	240	TACE, RFA	HBV	Yes	A	1.4	No	10.3	1	1
Male	72	Naïve		None	HBV	Yes	A	2.7	No	271.0	2	2
Female	77	Naïve		None	HBV	Yes	A	7.4	Yes	562.0	3	2
Male	69	Recurred	427	Resection	HBV	Yes	A	2.7	No	10.6	3	2
Female	83	Naïve		None	Non-viral	Yes	B	5.8	No	53.1	3	2

Abbreviations: TACE, Transarterial chemoembolization; RFA, radiofrequency ablation; HBV, hepatitis B virus; AFP, alpha-fetoprotein.

https://doi.org/10.2147/JHC.S575861

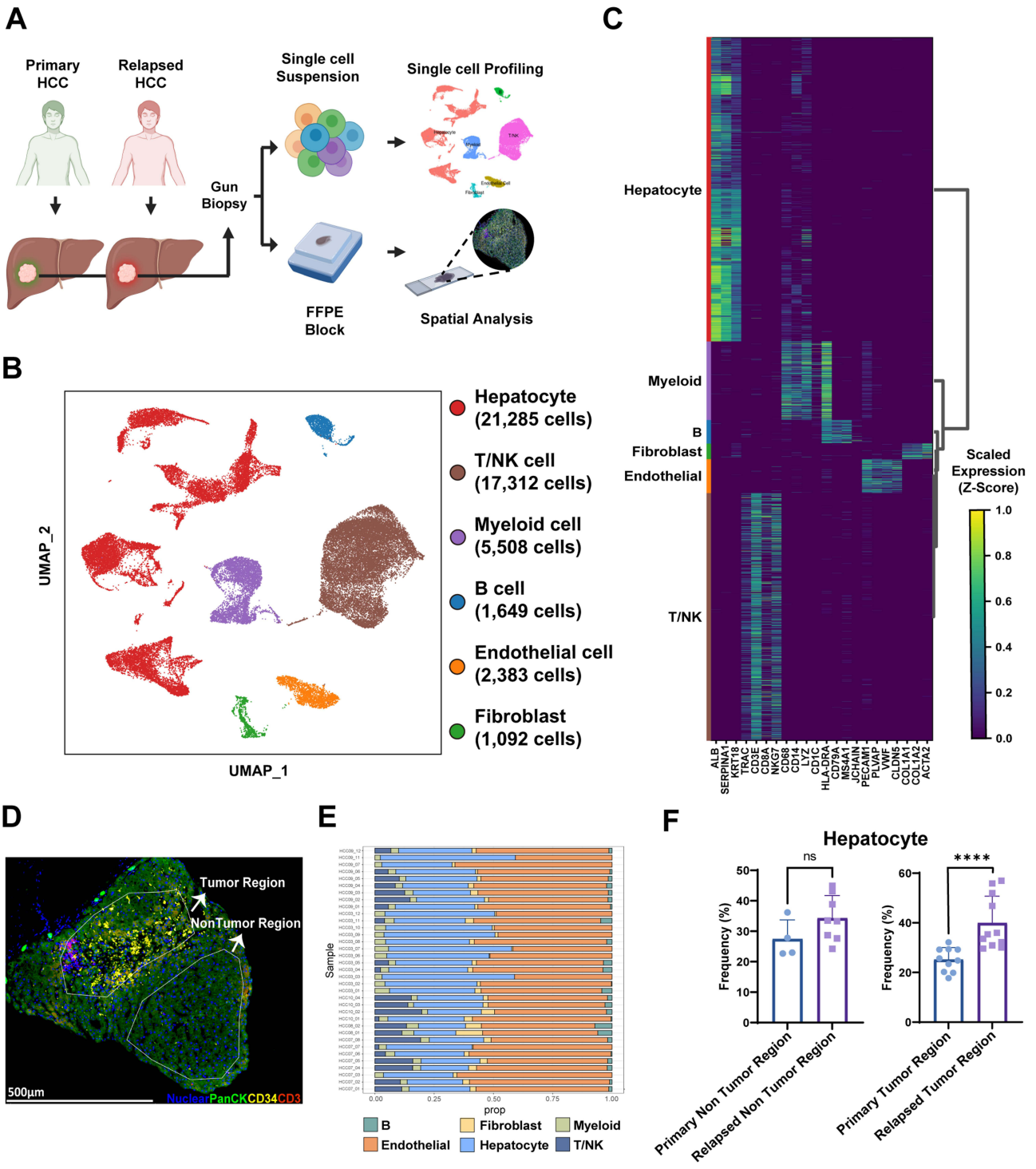

Figure 1 scRNA-seq and spatial transcriptomics profiling of cellular components in primary and relapsed HCC tumor tissues.Schematic overview of the experimental workflow for scRNA-seq and GeoMx spatial transcriptomic profiling of HCC tumor tissues (**A**). Uniform Manifold Approximation and Projection (UMAP) visualization of 49,229 single cells from five independent HCC patients, colored according to major cell types annotated based on canonical marker gene expression in scRNA-seq (**B**). Heatmap showing the expression of canonical marker genes used to define each major cell type in the scRNA-seq dataset (**C**). Representative immunofluorescence (IF) images of HCC tumor sections highlighting tumor and adjacent non-tumor regions (**D**). Estimated proportions of major cell types for each region of interest (ROI) derived from spatial transcriptomic data using cell type deconvolution based on scRNA-seq reference profiles (**E**). Bar plot showing differences in hepatocyte proportions between primary and relapsed tumors across tumor and non-tumor regions, calculated from deconvolved spatial transcriptomic data; statistical significance was assessed using the Mann–Whitney *U*-test (**F**). ****P ≤ 0.0001.

Abbreviation: ns, no significance.

https://doi.org/10.2147/JHC.S575861

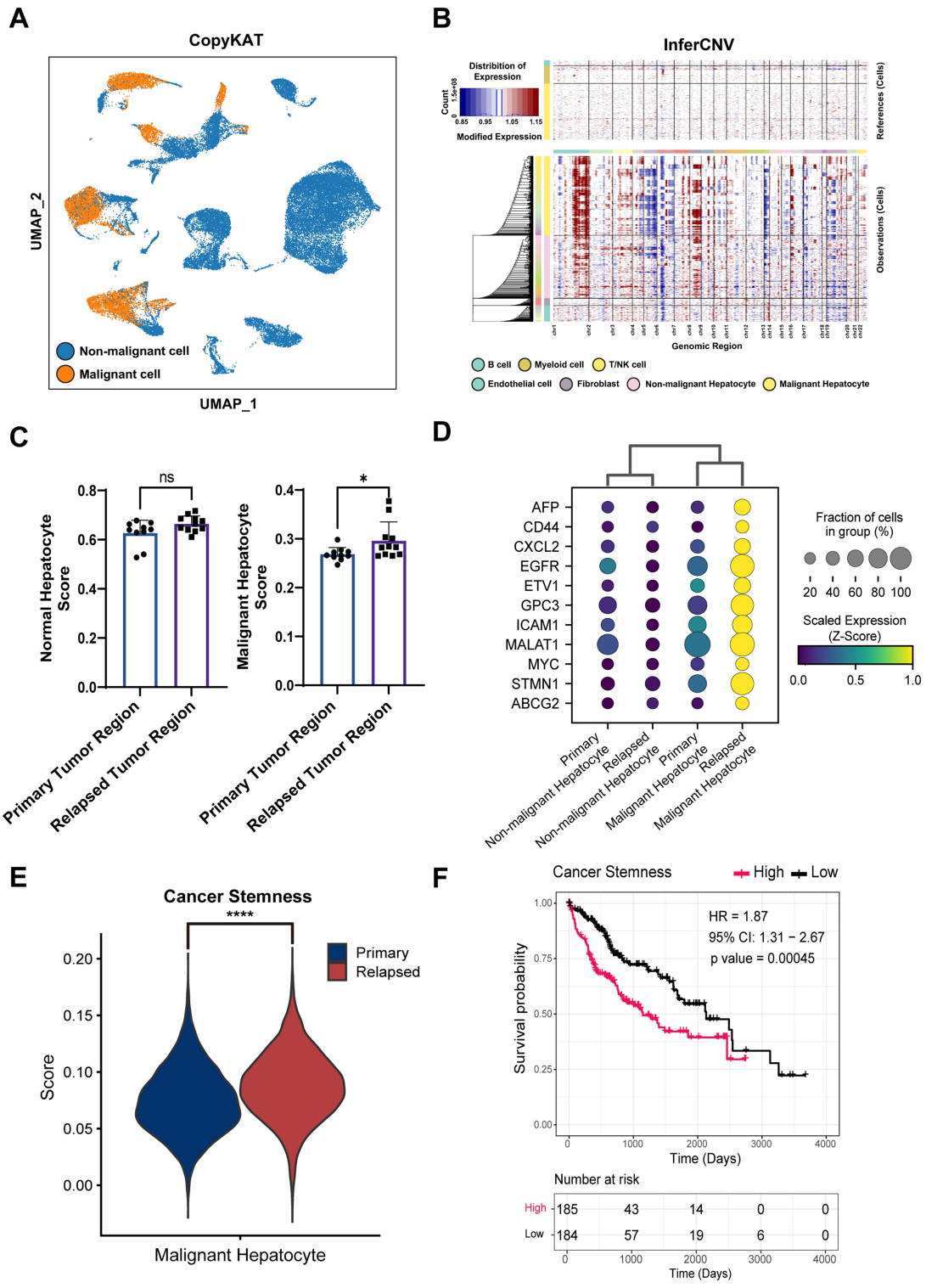

Figure 2 Enriched cancer stemness properties of malignant hepatocytes in relapsed HCC.UMAP plot of 49,229 single cells colored by malignant and non-malignant status as inferred using CopyKat-based copy number variation (CNV) analysis (**A**). Heatmap displaying inferred CNV profiles across chromosomes for each major cell type, distinguishing malignant hepatocytes from non-malignant populations (**B**). Bar plot showing enrichment scores of normal and malignant hepatocytes across tumor groups and tissue locations calculated from spatial transcriptomic data. (**C**). Dot plot illustrating the expression of stemness-related genes that were differentially expressed between malignant and normal hepatocytes, stratified by primary and relapsed tumors (**D**). Violin plot showing cancer stemness signature scores in malignant hepatocytes from primary versus relapsed tumors; statistical significance was determined using an unpaired *t*-test (**E**). Kaplan–Meier survival analysis of the TCGA-LIHC cohort (n = 369), stratified by high versus low cancer stemness scores (**F**). *P ≤ 0.05; ****P ≤ 0.0001.

Abbreviation: ns, no significance.

https://doi.org/10.2147/JHC.S575861

with tumor recurrence and poor prognosis in various cancer types including HCC.[24] Indeed, from TCGA LIHC database (n=369), patients with high cancer stemness property had poorer prognosis (HR=1.87, P < 0.001) (Figure 2F).

To further validate these findings in an independent cohort with a larger sample size, we performed additional analyses using a publicly available scRNA-seq dataset of HCC.[6] This dataset comprises single-cell transcriptomic profiles from tumor regions and adjacent non-tumor regions of 18 HCC patients, including 12 primary HCC and 6 relapsed HCC cases. We reprocessed the dataset and performed clustering in a manner closely aligned with the original study. Broad cell type annotation was conducted based on canonical marker expression, identifying six major cell populations: hepatocytes, T/NK cells, myeloid cells, B cells, endothelial cells, and fibroblasts, consistent with our own dataset (Supplementary Figure 2E and F; Supplementary Table 6). Using the CancerSEA stemness gene set, we calculated stemness scores specifically in hepatocytes from this independent cohort. Consistent with our observations, hepatocytes from relapsed tumor regions exhibited significantly higher cancer stemness scores compared with those from primary tumors (1.14-fold change, p value < 0.0001) (Supplementary Figure 2G). These data suggest that relapsed tumors are enriched in malignant hepatocytes with high stemness properties, which are associated with tumor recurrence and poor prognosis in HCC.

Increased Abundance of MAIT Cells in the Tumor Microenvironment of Relapsed HCC

Cross-talk between cancer cell and their surrounding TME plays a pivotal role in maintaining cancer cell stemness.[25] Tumor-infiltrated lymphocytes within the TME can promote cancer stemness by secreting various chemokines such as CCL5, IL-1B, IL-6, and TGF-β.[26] IF imaging showed the proximal localization of T cells to tumor cells, suggesting their possible interaction within the TME (Figure 3A). To investigate this, we performed sub-clustering of the T/NK cluster and identified 13 distinct subsets based on their gene expression levels using scRNA-seq (Figure 3B and C and Supplementary Figure 3A). When comparing the distribution of T/NK subsets between primary and relapsed tumors, MAIT cells appeared more prevalent in relapsed tumors (Supplementary Figure 3B and Supplementary Table 7).

To identify specific T cell subsets potentially involved in regulating the enriched cancer stemness properties of malignant hepatocytes in relapsed tumors, we conducted cell-to-cell interaction analysis using the CellPhoneDB package. Interestingly, cell-cell interaction analysis between malignant hepatocytes and each T cell subset revealed that malignant hepatocytes had enriched interactions with MAIT cells compared to other T cell subsets (Figure 3D).

In addition, we scored a MAIT cell signature gene set identified from scRNA-seq data for spatial transcriptomic data to compare its enrichment within tumor tissues between primary and relapsed tumors (Supplementary Figure 3C and Supplementary Table 8). MAIT cells were significantly enriched in the relapsed tumor compared to the primary tumor in tumor region (2.71-fold change than primary tumor regions, p≤0.05) (Figure 3E and Supplementary Table 9).

To further validate the observed enrichment of MAIT cells in relapsed tumors, we analyzed an independent public scRNA-seq dataset of HCC.[5] We re-analyzed the T/NK cell population and performed unsupervised sub-clustering, identifying 17 distinct subsets (Supplementary Figure 2E and 3D and Supplementary Table 10). To align these subsets with our dataset, we generated a signature gene sets for each subset from our T/NK population based on their DEGs and applied signature scoring across the public T/NK subsets (Supplementary Table 11). This analysis identified cluster 15 as the subset most closely resembling MAIT cells in our dataset (Supplementary Figure 3E). Frequency comparison demonstrated that the cluster 15 was more prevalent in relapsed tumor regions compared to primary tumor regions (2.84-fold change, p≤0.05) (Supplementary Figure 3F). Collectively, these findings suggest that MAIT cells are relatively enriched in relapsed HCC tumors and may preferentially interact with malignant hepatocytes, raising the possibility that MAIT cell–tumor cell interactions are associated with the altered tumor microenvironment and enhanced cancer stemness features observed in relapsed HCC.

Dysfunctional Transcriptional States of MAIT Cells and Their Association with Poor Prognosis in Relapsed HCC

To investigate the role of enriched MAIT cells in relapsed HCC, we compared the DEGs of MAIT cells between primary and relapsed tumors (Supplementary Table 12 and 13). MAIT cells in primary tumors enhanced the expression of

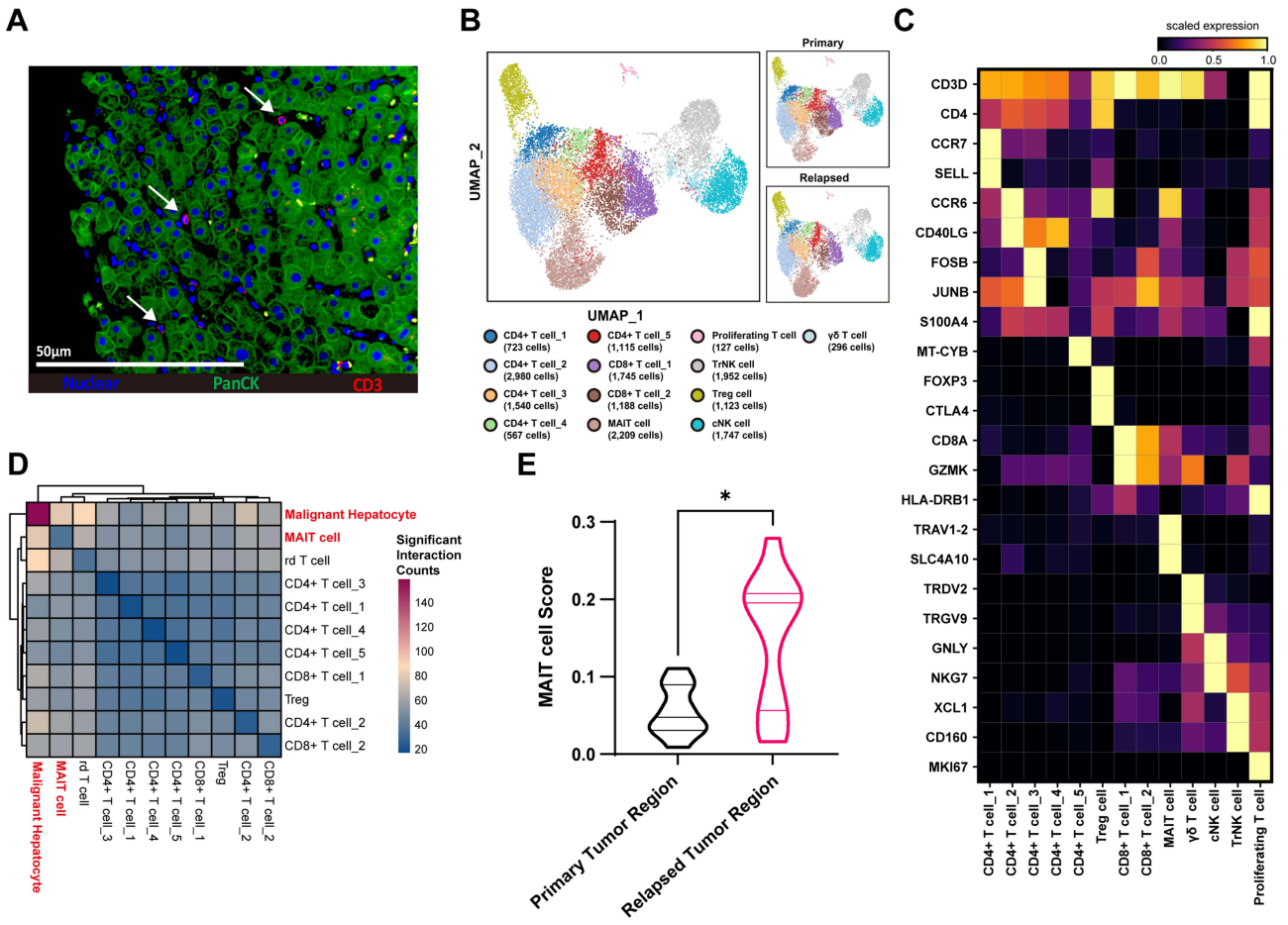

Figure 3 TNK subsets profiling showed increased MAIT cell in relapsed HCC tumor tissue.Immunofluorescence (IF) images showing the spatial proximity of T cells (CD3) to tumor cells (PanCK), suggesting potential interactions within the tumor microenvironment. White arrows highlight representative areas of close spatial proximity between T cells and tumor cells (**A**). UMAP visualization of 17,312 T/NK cells from scRNA-seq data, colored by transcriptionally defined T/NK subsets identified through unsupervised clustering (**B**). Pseudobulk heatmap showing differentially expressed marker gene expression across the T/NK cluster subsets (**C**). Heatmap showing the number of statistically significant ligand–receptor interactions between malignant hepatocytes and each T/NK subset, inferred using CellPhoneDB; only interactions passing significance thresholds were counted (**D**). Violin plot showing MAIT cell enrichment scores derived from spatial transcriptomic data in primary versus relapsed tumors; statistical significance was assessed using the Mann–Whitney *U*-test (**E**). *P ≤ 0.05.

Abbreviation: TrNK cells, tissue-resident NK cells; Treg cells, regulatory T cells; cNK cells, circulating NK cells; γδ T cells, gamma delta T cells.

inflammation-related genes including GNLY, TNF, IFNG, CD40LG, and GZMH (Figure 4A). In contrast, relapsed tumor MAIT cells showed upregulation of CXCR4, CCR6, TGFB1, and WNT1. Gene Ontology pathway analysis of each MAIT cell DEGs revealed distinct functional profiles. In relapsed tumors, MAIT cells downregulated inflammation-related pathways including T cell receptor signaling, type II interferon production, and leukocyte chemotaxis. Conversely, MAIT cells in primary tumors were associated with immune responses targeting the tumor cells (Figure 4B). Downregulation of these pathways—including T cell receptor signaling, type II interferon production, and leukocyte chemotaxis—has been reported to be associated with reduced anti-tumor immune activity.[11,27,28] In this context, the observed transcriptional changes indicate that MAIT cells in relapsed HCC are characterized by gene expression patterns linked to diminished anti-tumor immune responses.

Next, we examined the interactions between MAIT cells and malignant hepatocytes in both primary and relapsed tumors (Supplementary Tables 14 and 15). Cell-to-cell interaction analysis revealed enriched ligand–receptor pairs involving WNT1, TGFB1, and amphiregulin (AREG) between malignant hepatocytes and MAIT cells in relapsed tumors (Figure 4C). These ligand–receptor pairs have been previously implicated in pathways related to cancer cell proliferation and stemness, and their enrichment was accompanied by increased Wnt signaling activity in relapsed tumor regions (Supplementary Figure 2C and D).[29–31] Consistent with this observation, WNT1 expression was predominantly detected

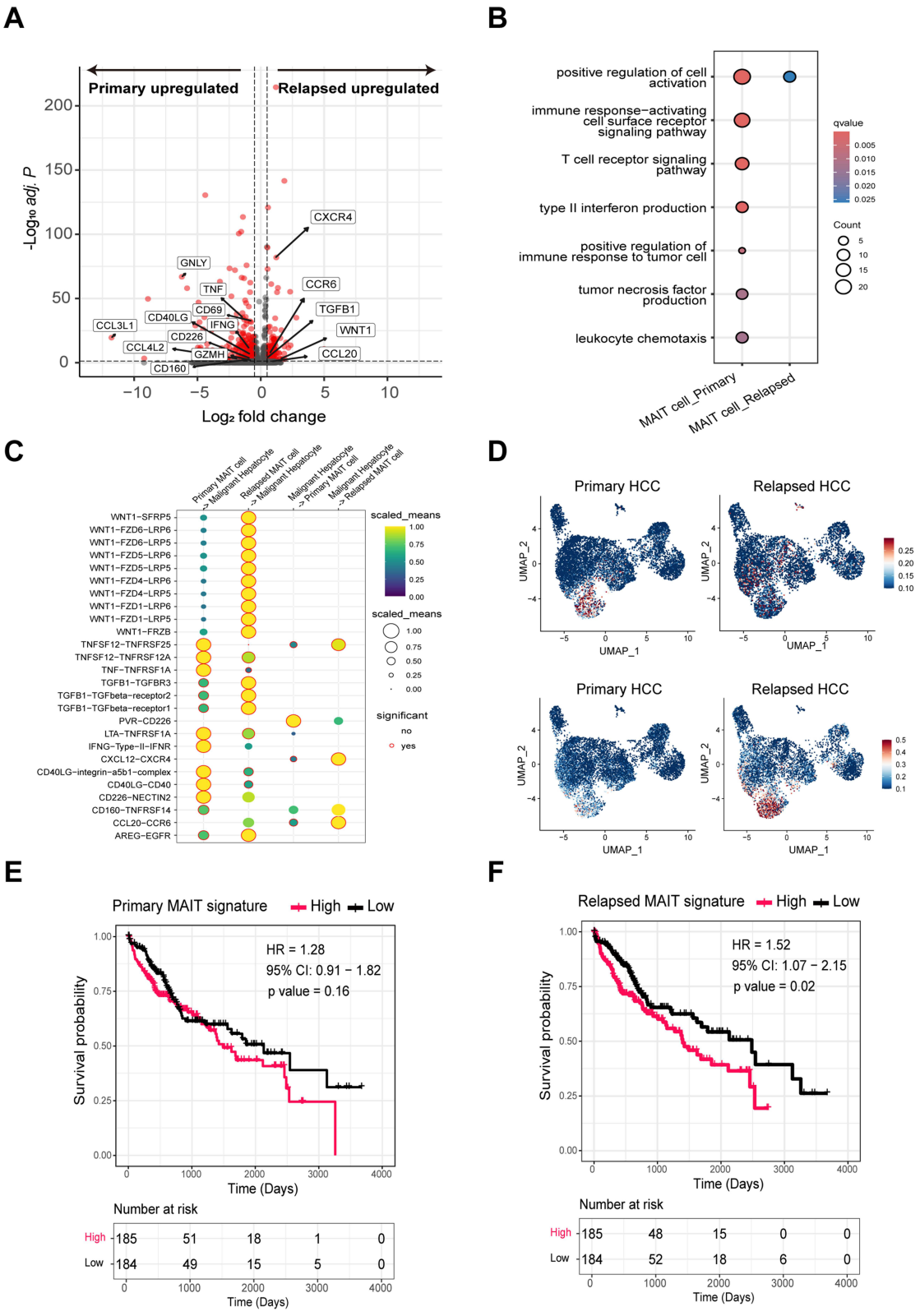

Figure 4 Altered MAIT cell transcriptional features in relapsed tumors and association with patient prognosis.Volcano plot showing differentially expressed genes (DEGs) between MAIT cells from primary and relapsed tumors identified from scRNA-seq data (**A**). Dot plot showing downregulated Gene Ontology (GO) pathways in relapsed MAIT cells compared with primary MAIT cells (**B**). Bubble chart illustrating differences in predicted ligand–receptor interactions between malignant hepatocytes and MAIT cells in primary versus relapsed tumors, inferred using CellPhoneDB (**C**). UMAP plots showing primary (upper row) and relapsed (lower row) MAIT cell signature gene set scores projected onto T/NK subsets (**D**). Kaplan–Meier survival analyses of the TCGA-LIHC cohort (n = 369), comparing patients with low versus high primary MAIT cell signatures (**E**) or relapsed MAIT cell signatures (**F**).

https://doi.org/10.2147/JHC.S575861

in MAIT cells within HCC tumor tissues (Supplementary Figure 4A and B). CXCL12-CXCR4 and CCL20-CCR6 interactions were upregulated in relapsed tumors, potentially explaining enhanced MAIT cell infiltration (Figure 3E).[32,33] In particular, high expression of CCL20 in HCC was associated with poorer recurrence-free survival rate.[34] In contrast, interactions associated with inflammation and anti-tumor immunity such as TNF-, IFNG-, CD40LG-CD40, and PVR-CD226 were enriched between malignant hepatocytes and MAIT cells in primary tumors (Figure 4C).

We next examined MAIT-cell–specific transcriptional programs in a public scRNA-seq dataset of HCC. As described above, we focused on cluster 15, which corresponded to MAIT cells (Supplementary Figure 3E). Using the gene set upregulated in relapsed MAIT cells compared with primary MAIT cells in our cohort, we performed gene signature scoring in this independent dataset and compared scores across groups (Supplementary Table 13). Consistent with our findings, MAIT cells from relapsed tumor regions exhibited significantly higher signature scores than those from primary tumors in the public dataset (1.24-fold change, $p<0.0001$) (Supplementary Figure 4C). Notably, this difference was not observed in MAIT cells from adjacent non-tumor liver tissues, indicating that the altered transcriptional state of relapsed MAIT cells is tumor-specific. Together, these results from an independent cohort further validate that relapsed HCC is characterized by functionally altered MAIT cells within the tumor microenvironment.

To explore the prognostic relevance of MAIT cells, we defined MAIT cell signature gene sets to discriminate MAIT cells between primary and relapsed tumors (Figure 4D and Supplementary Table 16, and 17). These signature gene sets were determined by the combination of MAIT cell cluster DEGs within TNK cell cluster and DEGs in MAIT cells between primary and relapsed tumors. Using TCGA data, we stratified the patients into high and low groups based on the gene sets. While the primary MAIT cell high and low groups did not show significant differences in prognosis ($HR=1.28$, $p>0.05$) (Figure 4E), the relapsed MAIT cell high group exhibited significantly poorer prognosis ($HR=1.52$, $p\leq0.05$) (Figure 4F).

To further assess whether this association was independent of established clinical variables, we performed multivariate Cox proportional hazards analysis incorporating age, sex, tumor grade, and hepatitis B virus (HBV) infection status. Consistent with the univariate analysis, the primary MAIT cell signature was not significantly associated with patient prognosis ($HR = 1.50$, $p = 0.10$). In contrast, a high relapsed MAIT cell signature remained significantly associated with worse overall survival ($HR = 2.18$, $p = 0.004$) (Supplementary Figure 4D and E). Collectively, our results indicate that MAIT cells in relapsed HCC display altered, dysfunctional features that are associated with poorer clinical outcomes. These observations suggest a potential contribution of MAIT cell dysregulation to the immune landscape of relapsed HCC.

Discussion

Cancer stemness, defined by the stem cell-like phenotypes of cancer cells, critically influences tumor progression, chemoradiotherapy resistance, recurrence, and metastasis in malignancies, including HCC.[35] Increased cancer stemness markers (CD133, EPCAM, CD44) associates with recurrence and poor survival in HCC.[24,36] Recent scRNA-seq advances identified stemness-enriched subpopulations linked to poor HCC prognosis.[37] Our integrated scRNA-seq and spatial transcriptomic analyses revealed an increased representation of malignant hepatocytes with elevated stemness-related transcriptional programs in relapsed HCC compared with primary tumors. Spatial transcriptomics further demonstrated enrichment of Wnt signaling pathways in relapsed tumor regions, supporting a spatially stemness-promoting microenvironment.[23] While these findings do not establish causality, they indicate that relapsed HCC is characterized by a transcriptionally distinct tumor state associated with aggressive biological features.

Accumulating evidence indicates that the tumor microenvironment (TME) plays a key role in regulating cancer stemness through paracrine signaling from stromal and immune cells.[38] Cancer-associated fibroblast (CAF)-secreted factors have been shown to promote stemness across cancers. In particular, WNT5A derived from SLC14A1+ CAF induces cancer stemness through the β-catenin pathway.[39] Beyond stroma cells, diverse immune cell populations including T cells, macrophages, and neutrophils are also implicated as key sources of cancer stemness-promoting signals.[40–42] In this context, our analyses suggest that MAIT cells undergo relapse-associated transcriptional reprogramming within the tumor microenvironment. Compared with primary tumors, MAIT cells in relapsed HCC exhibited reduced expression of effector-associated genes and pathways involved in T cell receptor signaling, interferon responses, and leukocyte chemotaxis, consistent with a dysfunctional immune state. Concurrently, relapsed MAIT cells upregulated

transcripts encoding WNT1, TGFB1, and AREG—ligands implicated in cancer stemness and tumor cell plasticity alongside possible interactions with malignant hepatocytes.[29–31] These observations support a model in which MAIT cells in relapsed tumors reside within an immune environment marked by reduced anti-tumor activity and transcriptional programs that are associated with tumor stemness. Importantly, these conclusions are based on transcriptional inference and predicted ligand–receptor interactions and therefore warrant future functional validation.

The mechanisms underlying MAIT-cell dysfunction in relapsed HCC are likely shaped by the local tumor microenvironment rather than intrinsic MAIT-cell properties. Previous studies have shown that tumor-associated macrophages, inhibitory checkpoint signaling, and cytokine imbalance can suppress MAIT-cell effector function in HCC, and that MAIT-cell activity is highly sensitive to local cytokine cues such as IL-7.[13,43] In line with these observations, MAIT-cell transcriptional alterations in our study were largely confined to tumor regions, while adjacent non-tumor liver tissues showed relatively preserved MAIT-cell profiles. This spatial restriction suggests that relapse-associated MAIT-cell dysfunction reflects tumor-conditioned immune remodeling rather than systemic immune alteration.

Our findings also provide a framework to reconcile previously conflicting reports regarding the prognostic significance of MAIT cells in HCC. Earlier studies have relied either on flow cytometric quantification of MAIT-cell abundance or on bulk transcriptomic MAIT-related gene signatures, yielding opposing survival associations.[11–13] By defining MAIT-cell states at single-cell resolution and constructing relapse-specific MAIT gene signatures, we demonstrate that prognostic relevance depends on disease-stage–specific transcriptional programs rather than MAIT-cell abundance alone. Notably, only the relapsed MAIT-cell signature not the primary MAIT-cell signature was associated with adverse survival in independent cohorts, highlighting the importance of functional state and disease context.

Several limitations should be considered in our study. First, the cohort size was small, which limits statistical power and may differentially affect analyses of rare cell populations and interaction inference. While concordant findings across scRNA-seq, spatial transcriptomics, and external validation datasets support robustness, subtle subtype-specific effects may have been missed. Second, most patients had HBV-associated HCC, which is known to influence MAIT-cell biology. Although HBV etiology was balanced between primary and relapsed groups, we cannot fully exclude etiologic effects, underscoring the need for validation in larger, etiology-diverse cohorts. Third, biopsy-based spatial transcriptomics is inherently susceptible to sampling bias due to intratumoral heterogeneity. Although multiple cores and standardized sampling were used, spatial conclusions should be interpreted as region-specific rather than tumor-wide. Finally, our study is descriptive in nature; functional assays will be required to directly test whether relapse-associated MAIT-cell states causally contribute to tumor stemness or recurrence.

From a translational perspective, although our data suggest that MAIT-cell dysfunction is associated with relapse-specific tumor biology, direct therapeutic targeting of MAIT cells poses challenges. MAIT cells play essential roles in mucosal immunity, and systemic depletion could carry significant safety risks.[44] Our findings instead support the concept that selectively modulating tumor-conditioned MAIT-cell states or the signaling pathways governing their interaction with malignant hepatocytes may represent a more feasible strategy. Importantly, while the present study focuses on MAIT-cell alterations within the tumor microenvironment, future investigations incorporating peripheral blood samples from primary and relapsed HCC patients may reveal systemic immunological changes associated with relapse. They could potentially be integrated with established relapse biomarkers, such as alpha-fetoprotein (AFP) levels or circulating tumor DNA, to improve risk stratification and disease monitoring, while also providing an immune-related component that current markers may not capture. Further mechanistic and longitudinal studies will be necessary to determine whether MAIT-cell–associated transcriptional programs can serve as reliable biomarkers or therapeutic entry points in recurrent HCC.

Conclusion

In this study, we integrated single-cell RNA sequencing and spatial transcriptomics to delineate cellular and transcriptional features associated with relapsed HCC, using paired analyses across independent patient cohorts. Rather than identifying a single dominant driver, our results highlight coordinated changes in both malignant hepatocytes and immune components within the relapsed tumor microenvironment. Relapsed tumors were characterized by an increased representation of malignant hepatocytes exhibiting transcriptional programs associated with cancer stemness, alongside altered MAIT cell states with dysfunctional phenotypes. Importantly, these observations are derived from transcriptomic

and spatial associations and should be interpreted as correlative. MAIT cell dysregulation is therefore unlikely to act in isolation, but instead represents one element within a broader network of immune and non-immune interactions that collectively accompany tumor relapse. From a translational perspective, our findings suggest that relapse-associated immune remodeling may not be fully captured by tumor-intrinsic features alone. However, the clinical relevance of MAIT cell states in this context remains to be determined. Future studies should focus on validating these observations at the protein and functional levels, including spatially resolved protein expression, perturbation based in vitro assays, and longitudinal sampling to assess temporal dynamics during relapse. Such efforts will be necessary to clarify whether altered MAIT cell states actively contribute to relapse-associated tumor biology or reflect downstream consequences of tumor evolution. Overall, this work provides a systems-level framework for understanding immune and tumor cell heterogeneity in relapsed HCC and offers hypotheses for future mechanistic and translational studies, rather than definitive therapeutic conclusions.

Abbreviations

AREG, amphiregulin; CAF, Cancer-associated fibroblasts; CNV, Copy number variation; DEGs, Differentially expressed genes; DSP, Digital Spatial Profiling; FBS, Fetal Bovine Serum; GO, Gene Ontology; GSEA, Gene Set Enrichment Analysis; H&E, hematoxylin and eosin; HCC, Hepatocellular carcinoma; IF, immunofluorescence; MAIT, mucosal-associated invariant T cells; PCA, Principal component analysis; QC, quality control; ROI, Regions of Interest; scRNA-seq, single-cell RNA sequencing; TAMs, tumor-associated macrophages; TCGA, The Cancer Genome Atlas; TME, tumor microenvironment; UMAP, Uniform Manifold Approximation and Projection for Dimension Reduction.

Funding

This work was supported by the Bio & Medical Technology Development Program of the National Research Foundation (NRF) funded by the Korean government (MSIT) (No. RS-2022-NR067309). It was also partly supported by the Institute of Information & Communications Technology Planning & Evaluation (IITP) grant funded by the Korea government (MSIT) (No. RS-2021-II211343, Artificial Intelligence Graduate School Program, Seoul National University). Additionally, a research grant from Seoul National University College of Medicine (Grant No. 800-20220131) and funding from the Korean ARPA-H Project through the Korea Health Industry Development Institute (KHIDI), funded by the Ministry of Health & Welfare, Republic of Korea (Grant No. RS-2024-00512120), supported this study. This work was supported by Seoul National University Bundang Hospital – Basic Medical Science Joint Research Program (grant no. 16-2024-0009).

Disclosure

The authors report no conflicts of interest in this work.

References

1. Bray F, Laversanne M, Sung H, et al. Global cancer statistics 2022: GLOBOCAN estimates of incidence and mortality worldwide for 36 cancers in 185 countries. *CA Cancer J Clin*. 2024;74(3):229–263.
2. Singal AG, Lampertico P, Nahon P. Epidemiology and surveillance for hepatocellular carcinoma: new trends. *J Hepatol*. 2020;72(2):250–261. doi:10.1016/j.jhep.2019.08.025
3. Tsilimigras DI, Bagante F, Moris D, et al. Recurrence patterns and outcomes after resection of hepatocellular carcinoma within and beyond the barcelona clinic liver cancer criteria. *Ann Surg Oncol*. 2020;27(7):2321–2331. doi:10.1245/s10434-020-08452-3
4. Safri F, Nguyen R, Zerehpooshnesfchi S, George J, Qiao L. Heterogeneity of hepatocellular carcinoma: from mechanisms to clinical implications. *Cancer Gene Ther*. 2024;31(8):1105–1112. doi:10.1038/s41417-024-00764-w
5. Chen KA, Shuen TWH, Chow PKH. The association between tumour heterogeneity and immune evasion mechanisms in hepatocellular carcinoma and its clinical implications. *Br J Cancer*. 2024;131(3):420–429. doi:10.1038/s41416-024-02684-w
6. Sun Y, Wu L, Zhong Y, et al. Single-cell landscape of the ecosystem in early-relapse hepatocellular carcinoma. *Cell*. 2021;184(2):404–421.e16. doi:10.1016/j.cell.2020.11.041
7. Dong X, Wang F, Liu C, et al. Single-cell analysis reveals the intra-tumor heterogeneity and identifies MLXIPL as a biomarker in the cellular trajectory of hepatocellular carcinoma. *Cell Death Discov*.;7(1). 10.1038/s41420-021-00403-5
8. Zhou PY, Zhou C, Gan W, et al. Single-cell and spatial architecture of primary liver cancer. *Commun Biol*. 2023;6(1):1181. doi:10.1038/s42003-023-05455-0

9. Dusseaux M, Martin E, Serriari N, et al. Human MAIT cells are xenobiotic-resistant, tissue-targeted, CD161hi IL-17-secreting T cells. *Blood*. 2011;117(4):1250–1259. doi:10.1182/blood-2010-08-303339
10. Godfrey DI, Koay HF, McCluskey J, Gherardin NA. The biology and functional importance of MAIT cells. *Nat Immunol*. 2019;20(9):1110–1128. doi:10.1038/s41590-019-0444-8
11. Duan M, Goswami S, Shi JY, et al. Activated and exhausted MAIT cells foster disease progression and indicate poor outcome in hepatocellular carcinoma. *Clin Cancer Res*. 2019;25(11):3304–3316. doi:10.1158/1078-0432.CCR-18-3040
12. Huang W, Ye D, He W, He X, Shi X, Gao Y. Activated but impaired IFN-gamma production of mucosal-associated invariant T cells in patients with hepatocellular carcinoma. *J Immunother Cancer*. 2021;9(11):e003685. doi:10.1136/jitc-2021-003685
13. Ruf B, Bruhns M, Babaei S, et al. Tumor-associated macrophages trigger MAIT cell dysfunction at the HCC invasive margin. *Cell*. 2023;186(17):3686–3705e32. doi:10.1016/j.cell.2023.07.026
14. Su W, Ling Y, Yang X, Wu Y, Xing C. Tumor microenvironment remodeling after neoadjuvant chemoradiotherapy in local advanced rectal cancer revealed by single-cell RNA sequencing. *J Transl Med*. 2024;22(1):1037. doi:10.1186/s12967-024-05747-x
15. A KLC, K NCC. 2022 KLCA-NCC Korea practice guidelines for the management of hepatocellular carcinoma. *J Liver Cancer*. 2023;23(1):1–120.
16. Yang M, Song X, Zhang F, et al. Spatial proteomic landscape of primary and relapsed hepatocellular carcinoma reveals immune escape characteristics in early relapse. *Hepatology*.
17. Chen JL, Wang L, Li R, Jiao YF, Yu WF. High expression of endothelial progenitor cell-induced angiogenic markers is associated with bile acid levels in HCC. *Oncol Lett*. 2020;20(3):2729–2738. doi:10.3892/ol.2020.11815
18. Llovet JM, Kelley RK, Villanueva A, et al. Hepatocellular carcinoma. *Nat Rev Dis Primers*. 2021;7(1):6. doi:10.1038/s41572-020-00240-3
19. Mu X, Español-Suñer R, Mederacke I, et al. Hepatocellular carcinoma originates from hepatocytes and not from the progenitor/biliary compartment. *J Clin Invest*. 2015;125(10):3891–3903. doi:10.1172/JCI77995
20. Gao R, Bai S, Henderson YC, et al. Delineating copy number and clonal substructure in human tumors from single-cell transcriptomes. *Nat Biotechnol*. 2021;39(5):599–608. doi:10.1038/s41587-020-00795-2
21. Barkley D, Moncada R, Pour M, et al. Cancer cell states recur across tumor types and form specific interactions with the tumor microenvironment. *Nat Genet*. 2022;54(8):1192–1201. doi:10.1038/s41588-022-01141-9
22. Yuan HT, Yan M, Zhang GX, et al. CancerSEA: a cancer single-cell state atlas. *Nucleic Acids Res*. 2019;47(D1):D900–D908. doi:10.1093/nar/gky939
23. Chua HH, Tsuei DJ, Lee PH, et al. RBMY, a novel inhibitor of glycogen synthase kinase 3beta, increases tumor stemness and predicts poor prognosis of hepatocellular carcinoma. *Hepatology*. 2015;62(5):1480–1496. doi:10.1002/hep.27996
24. Tsui YM, Chan LK, Ng IO. Cancer stemness in hepatocellular carcinoma: mechanisms and translational potential. *Br J Cancer*. 2020;122(10):1428–1440. doi:10.1038/s41416-020-0823-9
25. Nallasamy P, Nimmakayala RK, Parte S, Are AC, Batra SK, Ponnusamy MP. Tumor microenvironment enriches the stemness features: the architectural event of therapy resistance and metastasis. *Mol Cancer*. 2022;21(1):225. doi:10.1186/s12943-022-01682-x
26. Dianat-Moghadam H, Sharifi M, Salehi R, Keshavarz M, Shahgolzari M, Amoozgar Z. Engaging stemness improves cancer immunotherapy. *Cancer Lett*. 2023;554:216007. doi:10.1016/j.canlet.2022.216007
27. Yan J, Allen S, McDonald E, et al. MAIT cells promote tumor initiation, growth, and metastases via tumor MR1. *Cancer Discov*. 2020;10(1):124–141. doi:10.1158/2159-8290.CD-19-0569
28. Chu TH, Ko CY, Tai PH, et al. Leukocyte cell-derived chemotaxin 2 regulates epithelial-mesenchymal transition and cancer stemness in hepatocellular carcinoma. *J Biol Chem*. 2022;298(10):102442. doi:10.1016/j.jbc.2022.102442
29. Katoh M, Katoh M. WNT signaling and cancer stemness. *Essays Biochem*. 2022;66(4):319–331. doi:10.1042/EBC20220016
30. Bellomo C, Caja L, Moustakas A. Transforming growth factor β as regulator of cancer stemness and metastasis. *Br J Cancer*. 2016;115(7):761–769. doi:10.1038/bjc.2016.255
31. Tung SL, Huang WC, Hsu FC, et al. miRNA-34c-5p inhibits amphiregulin-induced ovarian cancer stemness and drug resistance via downregulation of the AREG-EGFR-ERK pathway. *Oncogenesis*. 2017;6(5):e326. doi:10.1038/oncsis.2017.25
32. Ghanem I, Riveiro ME, Paradis V, et al. Insights on the CXCL12-CXCR4 axis in hepatocellular carcinoma carcinogenesis. *Am J Transl Res*. 2014;6(4):340–352.
33. Wang Y, Chen W, Qiao S, et al. Lipid droplet accumulation mediates macrophage survival and Treg recruitment via the CCL20/CCR6 axis in human hepatocellular carcinoma. *Cell. Mol. Immunol*. 2024;21(10):1120–1130. doi:10.1038/s41423-024-01199-x
34. Ding X, Wang K, Wang H, et al. High expression of CCL20 is associated with poor prognosis in patients with hepatocellular carcinoma after curative resection. *J Gastrointest Surg*. 2012;16(4):828–836. doi:10.1007/s11605-011-1775-4
35. Liu Q, Guo Z, Li G, et al. Cancer stem cells and their niche in cancer progression and therapy. *Can Cell Inter*. 2023;23(1):305. doi:10.1186/s12935-023-03130-2
36. Guo Z, Li LQ, Jiang JH, Ou C, Zeng LX, Xiang BD. Cancer stem cell markers correlate with early recurrence and survival in hepatocellular carcinoma. *World J Gastroenterol*. 2014;20(8):2098–2106. doi:10.3748/wjg.v20.i8.2098
37. Ho DW, Tsui YM, Sze KM, et al. Single-cell transcriptomics reveals the landscape of intra-tumoral heterogeneity and stemness-related subpopulations in liver cancer. *Cancer Lett*. 2019;459:176–185. doi:10.1016/j.canlet.2019.06.002
38. Loh JJ, Ma S. Hallmarks of cancer stemness. *Cell Stem Cell*. 2024;31(5):617–639. doi:10.1016/j.stem.2024.04.004
39. Ma Z, Li X, Mao Y, et al. Interferon-dependent SLC14A1(+) cancer-associated fibroblasts promote cancer stemness via WNT5A in bladder cancer. *Cancer Cell*. 2022;40(12):1550–1565.e7. doi:10.1016/j.ccell.2022.11.005
40. Sharma VP, Tang B, Wang Y, et al. Live tumor imaging shows macrophage induction and TMEM-mediated enrichment of cancer stem cells during metastatic dissemination. *Nat Commun*. 2021;12(1):7300. doi:10.1038/s41467-021-27308-2
41. Hwang WL, Lan HY, Cheng WC, Huang SC, Yang MH. Tumor stem-like cell-derived exosomal RNAs prime neutrophils for facilitating tumorigenesis of colon cancer. *J hematol oncol*. 2019;12(1):10. doi:10.1186/s13045-019-0699-4
42. Liu S, Zhang C, Wang B, et al. Regulatory T cells promote glioma cell stemness through TGF-β–NF-κB–IL6–STAT3 signaling. *Cancer Immunol Immunother*. 2021;70(9):2601–2616. doi:10.1007/s00262-021-02872-0
43. Tang XZ, Jo J, Tan AT, et al. IL-7 licenses activation of human liver intrasinusoidal mucosal-associated invariant T cells. *J Immunol*. 2013;190(7):3142–3152. doi:10.4049/jimmunol.1203218
44. Jabeen MF, Hinks TSC. MAIT cells and the microbiome. *Front Immunol*. 2023;14:1127588. doi:10.3389/fimmu.2023.1127588